Research Square

Preprints are preliminary reports that have not undergone peer review.
They should not be considered conclusive, used to inform clinical practice,
or referenced by the media as validated information.

Isolation and characterization of a novel bacteriophage infecting *Helicobacter pylori*

Sujeet Powar
Oita University
Tomohiro Miyoshi
Oita University
Ricky Indra Alfaray
Oita University
Batsaikhan Saruuljavkhlan
Oita University
Shinjiro Ojima
National Institute of Infectious Diseases, Japan Institute for Health Security
Michiyo Kataoka
National Institute of Infectious Diseases, Japan Institute for Health Security
Ho Dang Quy Dung
Cho Ray Hospital
Vu Van Khien
108 Central Hospital
Takako Osaki
Kyorin University School of Medicine
Tadaki Suzuki
National Institute of Infectious Diseases, Japan Institute for Health Security
Yoshio Yamaoka
Oita University
Kotaro Kiga
National Institute of Infectious Diseases, Japan Institute for Health Security
Hitomi Mimuro
mimuro@oita-u.ac.jp

Oita University

Article

Keywords: Helicobacter pylori, phage

Posted Date: April 6th, 2026

DOI: https://doi.org/10.21203/rs.3.rs-9144344/v1

License: This work is licensed under a Creative Commons Attribution 4.0 International License.
Read Full License

Additional Declarations: No competing interests reported.

Abstract

Helicobacter pylori is a gram-negative gastric pathogen associated with several gastric diseases, including cancer. Although prophage sequences are frequently detected in *H. pylori* genomes, only a limited number of active bacteriophages infecting this species have been analyzed, leaving phage–host interactions poorly understood. Here, we isolated and characterized a novel temperate bacteriophage, 418T1, from the *H. pylori* strain VN0418. Transmission electron microscopy revealed that 418T1 has a spherical head with a short tail. The phage exhibited a relatively broad host range, forming plaques on 67.6% of the tested strains. Notably, 418T1 remained stable across a wide pH range (pH 3–11), consistent with gastric adaptation. Genomic analysis revealed a 30,690 bp linear double-stranded DNA genome with direct terminal repeats, consistent with a T7-like fixed-end DNA packaging mechanism. Intergenomic similarity analysis classified 418T1 as a novel species within the genus *Schmidvirus*. Comparative genomics identified two tail protein genes unique to 418T1. Functional characterization revealed that one of these proteins, VN33, specifically binds to *H. pylori* cells only after cell-surface lipopolysaccharide (LPS) depletion, suggesting that its target is masked by LPS. Our findings expand the current knowledge of *H. pylori* bacteriophages and provide new insights into phage–host interactions.

Introduction

Helicobacter pylori is a gram-negative, microaerophilic bacterium that colonizes the stomach of approximately half of the world's population[1]. *H. pylori* infection plays a critical role in the development of chronic gastritis and other gastrointestinal diseases, such as gastric ulcer disease, gastric adenocarcinoma, and gastric mucosa-associated lymphoid tissue lymphoma[2,3]. The bacterium employs multiple virulence factors, such as motility, chemotaxis, and urease production, which facilitate successful colonization within the harsh gastric environment[4]. Although *H. pylori* infection is typically treated with antibiotics, the bacterium has rapidly developed resistance against commonly used antibiotic agents[5]. The emergence of antimicrobial and multidrug resistance among pathogenic bacteria has renewed global interest in alternative therapeutic strategies, including phage therapy.

Bacteriophages, or phages, are viruses that infect bacteria and represent the most numerous biological entities on Earth. Following bacterial infection, phages typically follow one of two life cycles: the lytic cycle or the lysogenic cycle. The lytic cycle is characterized by phage adsorption, genome replication, virion assembly, and bacterial lysis, whereas the lysogenic cycle involves the integration of the phage genome into the bacterial genome as a prophage[6]. In addition to their role as bacterial predators, bacteriophages influence bacterial pathogenicity and evolution through genome diversification via horizontal gene transfer[7].

Recent advances in sequencing technologies have enabled an in-depth analysis of the *H. pylori* genome, revealing the frequent presence of prophage sequences integrated into bacterial chromosomes[8]. Despite the detection of numerous prophage elements, only a limited number of *H. pylori* bacteriophages

have been experimentally isolated and characterized[9–12]. To date, only four plaque-forming *H. pylori* bacteriophages–KHP30[10], KHP40[11], Hpy1R[9] and 1961P[12]–have been described in detail. This suggests that *H. pylori* bacteriophages are severely underreported and understudied, given that the bacterium colonizes approximately half of the world's population. A more comprehensive understanding of *H. pylori* phages may provide insights into bacterial pathogenicity, adaptation, and potentially novel antibacterial strategies.

In this study, we report the isolation and characterization of a novel temperate bacteriophage, designated 418T1, from *H. pylori* strain VN0418. We describe its morphology, infection properties, genomic features, and the functional characterization of its tail proteins in host cell recognition. Our findings broaden the range of experimentally characterized *H. pylori* bacteriophages and provide new insights into their infection biology and host interactions.

Results

Isolation and basic characterization of bacteriophage 418T1

To identify the active bacteriophage infecting *H. pylori*, the culture supernatant of the clinical isolate VN0418[13] was examined for spontaneous phage release. The VN0418 strain was isolated from a 49-year-old male patient with a history of gastric cancer, and its genome has previously been sequenced[13]. Analysis of the VN0418 genome using PHASTER[14], a web server for identifying prophage regions in bacterial genomes, revealed the presence of an intact prophage region.

Prophage induction is commonly achieved by treatment with mitomycin C or ultraviolet (UV) irradiation. However, the VN0418 strain spontaneously releases phage particles into the culture medium (Fig. 1a). The phage was purified from a single plaque and subsequently propagated using the *H. pylori* strain TK1402m3C9 as the host strain. As shown in Fig. 1b, bacteriophage 418T1 formed clear plaques with a diameter of approximately 1–2 mm on this host strain.

To assess the host range of bacteriophage 418T1, plaque formation was examined using 37 *H. pylori* strains by spotting serially diluted phage suspensions (10^{10}– 10^{3} plaque-forming units (PFU)/mL) onto double-layer agar plates. At high phage titers, the 418T1 phage formed clear plaques on 25 strains (67.6%), indicating a relatively broad host range (Fig. 1c). In contrast, four strains (VN1281, VN0484, VN0324, and VN0443) exhibited only turbid plaques at the highest phage concentration. Therefore, these strains were considered weakly permissive rather than fully susceptible hosts. The accession numbers of the *H. pylori* strains used in this analysis are listed in Supplementary Table 1.

We further examined phage morphology using transmission electron microscopy. The 418T1 virion exhibited a spherical head with a short tail (Fig. 1d), with an average head diameter of 66.7 ± 3.0 nm

(mean ± standard deviation, n = 6). This morphology is similar to that of the previously reported *H. pylori* bacteriophages KHP30[15] and HPy1R[9].

Infection properties of bacteriophage 418T1 in H. pylori TK1402m3C9

The infection properties of bacteriophage 418T1 were examined using the *H. pylori* strain, TK1402m3C9 (Fig. 2). Adsorption kinetics were first assessed by quantifying the unadsorbed phage particles to bacterial cells over time. Approximately 35% of the input phage population was adsorbed to host cells within 40 min (Fig. 2a). A gradual decrease in adsorption was observed after this time point, indicating limited adsorption efficiency under the tested conditions.

The lytic activity of bacteriophage 418T1 was evaluated *in vitro* by infecting the strain TK1402m3C9 at different multiplicities of infection (MOIs) and monitoring bacterial growth by optical density (OD) at 600 nm (OD600). A reduction in OD was observed in an MOI-dependent manner: after 4 h at an MOI of 10, after 8 h at an MOI of 1, and after 12 h at an MOI of 0.1 (Fig. 2b). At higher MOIs (10 and 1), complete lysis of the bacterial culture was observed after 24 h, whereas complete lysis was not achieved at an MOI of 0.1.

The replication kinetics of bacteriophage 418T1 were further examined using a one-step growth curve assay. The phage exhibited a latent period of approximately 240 min, followed by a rise period resulting in a burst size of approximately 13 PFU per infected cell, as estimated from the difference between initial and plateau PFU values during the rise phase of the one-step growth curve (Fig. 2c).

The stability of bacteriophage 418T1 under different temperature conditions was evaluated. The phage remained infective following incubation at − 20°C, 4°C, 25°C, and 37°C (Fig. 2d). In contrast, the phage activity decreased at 42°C and was undetectable after incubation at 56°C (Fig. 2d). To evaluate pH stability, phage suspensions were incubated in Brucella broth adjusted to different pH values at room temperature for 60 min. The phage remained stable over a wide pH range, from pH 3 to pH 11 (Fig. 2e).

Chloroform sensitivity was further examined by treating phage suspensions with chloroform for 30 min at room temperature. No plaque formation was observed following chloroform treatment (Fig. 2f), indicating a loss of infectivity under these conditions.

Genomic features and comparative analysis of bacteriophage 418T1

The genome of bacteriophage 418T1 was sequenced using a combination of Illumina MiSeq and Oxford Nanopore sequencing. The phage genome consists of a linear double-stranded DNA molecule of 30,690 bp with a GC content of 35.7% (Fig. 3a). Direct terminal repeats of 550 bp were identified at both ends of the genome. Genome annotation using Pharokka[16] identified 38 open reading frames (ORFs), of which 25 were annotated as hypothetical proteins (Fig. 3a). The remaining ORFs included genes predicted to encode structural proteins, such as tail fiber proteins and the major head protein, as well as proteins

involved in transcriptional regulation and host cell lysis. No antibiotic resistance genes were detected in the 418T1 genome. Detailed annotation results are provided in Supplementary Table 2.

To assess whether bacteriophage 418T1 represents a novel species, its genome was compared with those of previously reported *Helicobacter* phages using intergenomic similarity analysis performed with the VIRIDIC[17] tool. Bacteriophage 418T1 exhibited nucleotide similarities of 77.6% to KHP40, 75.9% to 1961P, 76.8% to KHP30, and 72.7% to HPy1R (Fig. 3b). According to the ICTV species demarcation criteria, which define phage genomes sharing < 95% nucleotide similarity as different species, these values support the classification of 418T1 as a novel phage species. Notably, KHP30, KHP40, and HPy1R are members of the genus *Schmidvirus*, indicating that 418T1 represents a new species within this genus.

Identification and functional characterization of tail fiber proteins

A comparative genome alignment using the clinker[18] web server revealed the overall genomic organization of bacteriophage 418T1 and related *Helicobacter* phages (Fig. 4a). The genomes showed a largely conserved arrangement of ORFs, whereas several regions displayed low sequence similarity. Genes associated with structure and replication were highly conserved, whereas genes encoding hypothetical proteins of unknown function contributed predominantly to the variable regions.

Clear differences were observed in genes encoding tail proteins. The 418T1 genome contains two predicted tail protein genes, ZXOOZVVM_CDS_0026 and ZXOOZVVM_CDS_0027 (Supplementary Table 2), whereas phage HPy1R contains only a single homologous tail protein gene. These genes were not detected in other *Helicobacter* phage genomes analyzed (Fig. 4a).

To analyze the potential role of these tail proteins, ORFs ZXOOZVVM_CDS_0026 and ZXOOZVVM_CDS_0027 were designated VN32 and VN33, respectively. A global pairwise amino acid sequence alignment using EMBOSS NEEDLE revealed that VN32 (184 amino acids) and VN33 (222 amino acids) shared 66.5% amino acid identity and 70.0% similarity (Supplementary Fig. 1). Full-length VN32 and VN33 were expressed as N-terminal His-GFP fusion proteins, referred to as GFP-VN32 and GFP-VN33 full-length (FL), and purified using Ni-NTA affinity chromatography. GFP-VN32 was efficiently purified, whereas GFP-VN33 FL yielded lower amounts and displayed additional bands on SDS-PAGE, consistent with partial protein truncation (Fig. 4b and c, Supplementary Fig. 2).

To assess whether these proteins could bind to *H. pylori* cells, we examined the binding of GFP-fused proteins using fluorescence microscopy. Under standard conditions, neither GFP-VN32 nor GFP-VN33 FL showed detectable binding to bacterial cells (Fig. 5a).

To further evaluate the binding activity, bacterial cells were treated with sodium periodate to remove surface lipopolysaccharide (LPS), and the binding assay was repeated. Following LPS removal, GFP-

VN33 FL exhibited clear fluorescence signals on the bacterial surface, whereas GFP-VN32 remained negative (Fig. 5a).

To identify the regions of VN33 responsible for bacterial binding, we generated truncated versions of VN33 as GFP fusion proteins, corresponding to the N-terminal (amino acids 1–83; GFP-VN33 N-term) and C-terminal (amino acids 84–222; GFP-VN33 C-term) regions (Fig. 4b, Supplementary Fig. 3). Although GFP-VN33 N-term was efficiently purified, GFP-VN33 C-term showed partial truncation (Fig. 4c and Supplementary Fig. 2). When tested in binding assays using LPS-removed cells, neither truncated protein displayed detectable fluorescence signals (Fig. 5b), indicating that full-length VN33 protein is required for stable binding to the cell surface.

Discussion

Although prophage sequences are frequently detected in *H. pylori* genomes, only a limited number of experimentally tractable bacteriophages infecting this species have been reported to date. All previously characterized *H. pylori* phages were isolated from culture supernatants of bacterial strains, and none have been recovered from environmental sources. Consequently, fundamental aspects of *H. pylori* phage biology, including infection dynamics, host recognition mechanisms, and replication strategies, remain poorly understood. In this study, we isolated and characterized a novel temperate bacteriophage, 418T1, thereby expanding the currently limited repertoire of *H. pylori* phages available for experimental investigation and providing a new framework for mechanistic studies of phage–host interactions in this species.

A notable feature of bacteriophage 418T1 is its spontaneous release from the host strain VN0418 under standard *in vitro* growth conditions. Similar spontaneous phage release has been reported for most previously characterized *H. pylori* phages, suggesting that this mode of phage release may be a common trait within this group. In contrast, treatment with mitomycin C, a widely used inducer of SOS-mediated prophage activation, did not result in detectable plaque formation in our experimental system (data not shown). This observation does not necessarily indicate an absence of SOS responsiveness but rather highlights the limitations of prolonged mitomycin C exposure for evaluating productive phage infection in *H. pylori*. Continuous mitomycin C treatment is known to strongly inhibit host cell growth and viability, which likely interferes with subsequent phage propagation and plaque development. Consistent with this interpretation, short-pulse UV irradiation, which induces DNA damage while allowing partial host recovery, supported plaque formation comparable to that of untreated cultures (data not shown). Spontaneous prophage induction has been implicated in modulating bacterial fitness and virulence in several bacterial pathogens[19], its biological consequences in *H. pylori* remain largely unexplored. In this context, the spontaneous release of 418T1 provides an experimentally tractable system for investigating how prophage activation under physiological growth conditions may influence phage–host interactions in this species. Together, these findings suggest that spontaneous prophage induction, rather than chemically enforced induction, provides a more suitable context for assessing the productive infection cycle of 418T1. This mode of phage release may better reflect the physiological conditions under which

H. pylori prophages contribute to population-level dynamics without causing the immediate collapse of the host culture.

The infection dynamics of bacteriophage 418T1 reveal several features that distinguish it from well-studied lytic phages and are likely shaped by the unique biology of *H. pylori*. The adsorption of 418T1 to host cells was relatively inefficient, with only a fraction of the input phage population attaching within the first 40 min. Such limited adsorption efficiency may reflect restricted access to the phage receptor, heterogeneity in receptor expression, or interference by surface structures such as lipopolysaccharide, which is consistent with our subsequent binding assays using tail proteins. Despite inefficient adsorption, 418T1 was capable of productive infection at sufficiently high multiplicities of infection (MOI), as evidenced by MOI-dependent growth inhibition and lysis of *H. pylori* TK1402m3C9. This requirement for a high MOI suggests that successful infection relies on overcoming intrinsic barriers to phage entry or early replication, a phenomenon that has also been reported for other *H. pylori* phages. Notably, plaque formation by 418T1 was observed primarily at high phage titers, whereas little or no plaque formation occurred at lower input concentrations. In natural environments, phage titers are often low, and *H. pylori*, like many bacteria, is equipped with restriction-modification systems and other defense mechanisms that can limit productive infection[20]. These factors may further constrain plaque formation under low-titer conditions and contribute to the apparent requirement for a high MOI observed *in vitro*. One-step growth analysis further demonstrated that 418T1 exhibited a prolonged latent period of approximately 240 min and a modest burst size relative to those of many tailed bacteriophages. The combination of a prolonged latent period and a moderate burst size is consistent with a phage life cycle coordinated with the slow replication kinetics of *H. pylori*, rather than one optimized for rapid bacterial lysis. Together, these infection parameters suggest that 418T1 is optimized for persistence and gradual dissemination within *H. pylori* populations, rather than aggressive lytic propagation, which may be disadvantageous in the gastric niche.

Comparative genomic analysis revealed that bacteriophage 418T1 possesses a linear double-stranded DNA genome with short, exact direct terminal repeats (DTRs), a feature that distinguishes it from several previously characterized *H. pylori* phages[24]. Among the reported *H. pylori* phages, only 1961P shares a similar genome architecture with defined terminal repeats, whereas KHP30, KHP40, and HPy1R lack detectable terminal redundancy and exhibit alternative genome configurations. The presence of DTRs in 418T1 strongly suggests a T7-like DNA packaging strategy, in which genome maturation is guided by sequence-specific recognition and cleavage at defined termini. Diversity in genome topology and packaging strategies among *H. pylori* phages likely reflects evolutionary divergence driven by host-specific constraints rather than horizontal exchange with phages infecting fast-growing enteric bacteria. Given the compact genome size and limited repertoire of replication-associated genes, the adoption of a DTR-based packaging strategy may represent an efficient solution for genome encapsidation in a slow-growing host environment. Notably, despite sharing similar genome lengths, 418T1 and other *H. pylori* phages differ markedly in terminal structure, underscoring that genome size alone is insufficient to predict replication or packaging mechanisms. These findings highlight substantial mechanistic

heterogeneity among *H. pylori* bacteriophages and emphasize the importance of experimentally tractable isolates, such as 418T1, for expanding our understanding of phage genome organization in this clinically important pathogen.

The sensitivity of bacteriophage 418T1 to chloroform further suggests that this phage may contain lipid components within the virion. Lipid-containing bacteriophages have been reported for *H. pylori*, including phages 1961P and KHP30, as well as for diverse bacterial hosts[21]. In such phages, lipids play important roles at multiple stages of the phage life cycle, including virion stability, host entry, and genome delivery. A well-characterized example is bacteriophage PRD1, which forms an internal membranous tube that penetrates the host cell envelope and fuses with the cytoplasmic membrane, thereby enabling genome translocation into the host cytoplasm[22]. Although comparable mechanisms have not yet been described for *H. pylori* phages, the chloroform sensitivity of 418T1 raises the possibility that lipid components contribute to its infection process. At present, the functional role of lipids in *H. pylori* bacteriophage life cycles remains unclear and warrants further investigation.

A particularly distinctive feature of bacteriophage 418T1 is the presence of two predicted tail proteins, VN32 and VN33, which are absent in other characterized *H. pylori* phages. Functional analyses using GFP-tagged recombinant proteins revealed that neither GFP-VN32 nor GFP-VN33 FL bound to intact *H. pylori* cells. However, following chemical removal of surface LPS by sodium periodate treatment, GFP-VN33 FL clearly bound to bacterial cells, whereas GFP-VN32 did not bind. These results indicate that VN33 recognizes a host surface component that is normally masked by the LPS layer and becomes accessible only upon its removal. Notably, VN33 does not appear to possess LPS-depolymerase activity, distinguishing it from capsule- or LPS-degrading tail proteins described in other gram-negative bacteriophages.[23] Instead, our data suggest a two-step infection model in which initial phage attachment may occur through non-proteinaceous interactions with the bacterial surface, followed by engagement of a specific receptor by VN33 once steric hindrance by LPS is overcome. Such a mechanism is conceptually analogous to secondary receptor recognition systems reported for certain *Enterobacteriaceae* phages; however, it has not previously been described for *H. pylori* bacteriophages. Despite the high sequence similarity between VN32 and VN33 (Supplementary Fig. 1), neither the isolated N-terminal nor C-terminal domain of VN33 exhibited detectable binding to LPS-removed cells, indicating that full-length protein integrity and proper folding are required for receptor interaction. This observation suggests functional divergence following gene duplication, with VN33 evolving a specialized role in host recognition, while VN32 may fulfill a distinct function during phage assembly or infection. Together, these findings identify VN33 as a key determinant of host interaction in bacteriophage 418T1 and reveal a previously unrecognized mode of receptor accessibility and engagement in *H. pylori* phage infection.

Collectively, the characterization of bacteriophage 418T1 expands the current understanding of *H. pylori* bacteriophage biology and highlights both conserved and unique features within this group. While traits such as spontaneous release, acid stability, and a temperate lifestyle are shared with previously characterized *H. pylori* phages, the presence of two distinct tail proteins and a DTR-based genome

packaging strategy clearly distinguishes 418T1 from its relatives. Although the temperate nature of 418T1 limits its immediate applicability for phage therapy, this phage provides a valuable experimental model for dissecting phage–host interactions in *H. pylori*, a pathogen for which experimentally tractable phages remain extremely limited. In particular, the identification of VN33 as a host-interacting tail protein offers a concrete entry point for future studies aimed at defining bacterial receptors and elucidating mechanisms of phage entry in this species. Further investigation of the functional role of VN32, as well as exploration of strategies to engineer lytic derivatives of 418T1, may ultimately contribute to the development of phage-based approaches for studying and potentially controlling *H. pylori* infection.

Materials and Methods

Bacterial Strains, Phage, and Growth Conditions

H. pylori strains were cultivated on Tryptic Soy Agar plates supplemented with 5% sheep blood (BD BBL, Franklin Lakes, NJ, USA) under microaerophilic conditions at 37°C. For liquid cultures, bacteria were grown in Brucella broth (BD BBL, Franklin Lakes, NJ, USA) containing 5% fetal bovine serum (FBS; Corning, Arizona, USA) with shaking at 150 rpm at 37°C. The *H. pylori* strain TK1402m3C9 used in this study is a rodent-adapted clonal derivative of the parental strain TK1402. Other *H. pylori* strains used in this study are listed in Supplementary Table 1.

Prophage Induction and Phage Isolation

Exponentially growing *H. pylori* VN0418 cultures were incubated overnight. The lysates were centrifuged at 10,000 × *g* for 10 min at 4°C and filtered through 0.22 µm syringe filters (Ministart NML, SARTORIUS, Germany). The presence of phage particles was assessed by spotting serial dilutions of the filtrate onto agar plates overlaid with *H. pylori* strains. plates were then incubated at 37°C for 2–3 days. The 418T1 phage was purified by single-plaque isolation using the double-layer agar method with *H. pylori* TK1402m3C9 as the host strain.

The 418T1 bacteriophage was amplified on *H. pylori* TK1402m3C9 using the double-layer agar method. Briefly, a bacterial culture was mixed with the phage in 0.4% (w/v) soft agar prepared in Brucella broth supplemented with 10% FBS (Burucella soft agar) and poured onto Brucella agar plates containing 10% FBS. plates were incubated at 37°C under microaerophilic conditions for 24–48 h. After complete lysis, 6 mL of SM buffer (50 mM Tris-HCl pH 7.5, 100 mM NaCl, 7 mM $MgSO_4$, 0.01% gelatin) was added to the plates, followed by gentle rocking for 90 min. The overlay and SM buffer were collected and centrifuged at 10,000 × *g* for 10 min at 4°C. The supernatant was filtered through 0.22 µm syringe filters and stored at 4°C until use. Unless otherwise stated, the 418T1 bacteriophage was propagated using *H. pylori* TK1402m3C9 as the host.

For liquid amplification, *H. pylori* TK1402m3C9 cells were infected at an MOI of 1–2 and incubated with shaking at 150 rpm at 37°C under microaerophilic conditions until clear lysis was observed. The lysate

was centrifuged at 10,000 × *g* for 10 min at 4°C and filtered through 0.22 μm syringe filters.

Phage Host Range Determination

The host range of the 418T1 phage was determined against 37 *H. pylori* strains using a spot assay. Briefly, 2 μL of serially diluted phage in SM buffer (10^{10} to 10^{3} PFU/mL) was spotted onto a bacterial lawn prepared by mixing 500 μL of bacterial culture with 3 mL of Brucella soft agar. Plates were incubated under microaerophilic conditions at 37°C for 24–48 h. Host susceptibility was confirmed by the formation of clear plaques.

Transmission Electron Microscopy

Phage particles were concentrated using Amicon Ultra-15 centrifugal filters (100 kDa molecular weight cutoff, Merck Millipore, Burlington, MA, USA). The concentrated phage solution (3 mL) was layered on a CsCl step density gradient (1.46, 1.55, 1.63 g/mL) and centrifuged at 100,000 × *g* for 1 h at 4°C. The visible phage band was collected and dialyzed overnight at 4°C against SM buffer.

Negative staining transmission electron microscopy was performed as previously[24]. Briefly, purified phage particles (~ 10^{9} PFU/mL) were applied to Formvar and carbon-coated copper grids and allowed to adsorb for 1 min. Excess liquid was removed, and the grids were briefly rinsed with 20 μL of distilled water. Negative staining was performed using 2% uranyl acetate for 1 min. Grids were air-dried for 30 min and observed using a transmission electron microscope (HT7700, Hitachi Ltd., Japan) operated at 80 kV.

Phage Adsorption and Lytic Activity Assay

For the adsorption assays, 418T1 phage was mixed with *H. pylori* culture at an MOI of 0.001 in Brucella broth supplemented with 10 mM $MgSO_4$ and 2 mM $CaCl_2$. At the designated time points, the samples were centrifuged at 15,000 × *g* for 3 min, and the unadsorbed phages in the supernatant were quantified using a plaque assay.

For the lytic activity assays, bacterial cultures were infected with MOIs of 0.1, 1, and 10. Optical density (OD) at 600 nm (OD600) was measured every 4 h to monitor bacterial growth. Uninfected cultures were used as controls.

One-Step Growth Curve Assay

The latent period and burst size were determined using one-step growth assays. Logarithmic-phase bacterial cultures were adjusted to an OD600 of 0.1 and infected at an MOI of 0.1. After adsorption at 37°C for 30 min, cultures were then centrifuged (2150 × *g*, 10 min) to remove unadsorbed free phage and resuspended in fresh Brucella broth. The resuspended cultures were immediately incubated at 37°C with shaking at 150 rpm under microaerophilic conditions. Samples were collected immediately (t = 0 min) and at regular intervals up to 300 min. Phage titers were determined using a plaque assay. The latent

period was defined as the time interval between the start of incubation and the first detectable increase in phage titer. Burst size was calculated as follows:

Burst size = (Average titer at plateau − Average initial titer) / Average initial titer

The average initial titer was calculated from measurements at 120, 150, and 180 min (latent phase), and the plateau titer was calculated from measurements at 260 and 280 min (plateau phase).

Phage Stability Assays

pH stability was assessed as previously described previously[10]. 10 Brucella broth was adjusted to pH 1, 2, 3, 5, 7, 9, 11, and 13 by adding HCl or NaOH. The pH of the medium was checked using a pH meter. Phage suspensions were prepared in Brucella broth at different pH values and adjusted to a titer of 7.0×10^5 PFU/mL. The suspensions were then incubated at room temperature for 1 hour. Phage titers were then determined by plaque assay.

For thermal stability assessment, 1.0×10^5 PFU/mL of the 418T1 bacteriophage suspension was incubated for 1 h at − 20°C, 4°C, 25°C, 37°C, 42°C, or 56°C, and phage titers were then determined a plaque assay.

Chloroform sensitivity assay

Chloroform (200 µL; (Sigma-Aldrich, St. Louis, MO, USA) was added to the phage solution (10^9 PFU/mL), mixed well by vortexing, and incubated at room temperature for 30 min. After 30 min, the phage were collected, and 5 µL of the phage solution was spotted on a double-layer agar plate containing *H. pylori* TK1402m3C9 as the host strain.

Phage DNA Extraction

Approximately 20 mL of purified 418T1 phage suspension (1.0×10^9 PFU/mL) was used for DNA extraction. Polyethylene glycol (PEG) 8000 (MP Biomedicals, California, USA) was added to a final concentration of 10% (w/v), mixed thoroughly, and incubated overnight at 4°C. The mixture was centrifuged at 10,000 × *g* for 30 min at 4°C, and the supernatant was discarded. The pellet was resuspended in SM buffer (50 mM Tris–HCl pH 7.5, 100 mM NaCl, 8 mM $MgSO_4$) and treated with 1 µL DNase I (11 Units/µL; Nippon Gene, Tokyo, Japan) and 2.5 µL RNase A (10mg/mL; Nippon Gene) at 37°C for 60 min. Subsequently, 20 µL of 10% SDS (FUJIFILM Wako Pure Chemical Corporation, Osaka, Japan), 25 µL of 0.5 M EDTA (Dojindo Laboratories Co., Ltd., Kumamoto, Japan), and 5 µL proteinase K (20mg/mL; Sigma-Aldrich) were added, and the mixture was incubated at 60°C for 1 h. An equal volume of phenol:chloroform:isoamyl alcohol (25:24:1, v/v/v; Nippon Gene) was added, mixed, and centrifuged at 15,000 × *g* for 10 min. The aqueous phase was collected, extracted once with chloroform, and centrifuged again under the same conditions. Phage DNA was precipitated by adding 0.1 volume of 3 M sodium acetate (pH 5.2) and 2.5 volume of ice-cold 100% ethanol, followed by incubation at − 20°C for 1 h. The DNA pellet was collected by centrifugation, washed with 70% ethanol, air-dried, and dissolved in Milli-Q water (Merck Millipore, Burlington, MA, USA).

Phage Genome Sequencing and Annotation

The phage genome was sequenced using Illumina MiSeq (2 × 300 bp, paired-end; Illumina, San Diego, CA, USA) and Oxford Nanopore sequencing (Oxford Nanopore Technologies, Oxford, UK). The genome was assembled using Trycycler[25] and polished with Illumina reads using Polypolish[26]. The phage genome was annotated using Pharokka v1.3.0 with default parameters. Pharokka performs coding sequence (CDS) and tRNA predictions using PHANOTATE[27] and tRNAscan-SE 2.0[28] respectively. Pharokka further utilizes MMseqs2[29] to assign functional annotation by matching CDSs to PHROGs[30], VFDB[31], and CARD[32] databases. Whole-genome alignment was generated using the clinker[18] webserver. Intergenomic similarities among related phage genomes were calculated using the Virus Intergenomic Distance Calculator (VIRIDIC; http://rhea.icbm.uni-oldenburg.de/VIRIDIC/)[17].

Tail fiber protein cloning

Tail fiber protein coding sequences VN32 and VN33 were amplified from the 418T1 phage genomic DNA by PCR using primers. Primer sequences are described in Supplementary Table 3. The pET28a plasmid (Novagen, Madison, WI, USA) was digested with *Xho*I and *Nde*I restriction enzymes (New England Biolabs). The PCR products and digested plasmid were ligated using the NEBuilder HiFi DNA Assembly kit (New England Biolabs) and transformed into *E. coli* DH5α cells (SMOBIO, Technology, Inc., Taiwan).

Protein Expression and Purification.

An overnight culture of plasmid-transformed *E. coli* BL21(DE3) (SMOBIO, Technology, Inc.) was used to inoculate 100 mL of LB medium supplemented with 50 μg/mL kanamycin (FUJIFILM Wako) and grown with shaking at 37°C until OD600 reached 0.6. Protein expression was induced with 0.5 mM isopropyl-β-D-thiogalactopyranoside (IPTG; FUJIFILM Wako), and the cultures were incubated for 20 h with agitation at 23°C. Cells were harvested by centrifugation at 10,000 × *g* for 10 min at 4°C, resuspended in 6 mL of lysis buffer (50 mM Tris-HCl pH 8.0, 700 mM NaCl, 0.1% Triton X-100, with protease inhibitor cocktail; Roche Diagnostics, Basel, Switzerland), and lysed by sonication on ice (10 s on, 10 s off, for 10 min total). After centrifugation at 15,000 × *g* for 10 min, the supernatant was incubated with Ni-NTA agarose beads (QIAGEN, Hilden, Germany) at 4°C on a slow rotator. Beads were washed three times with washing buffer (50 mM Tris-HCl, pH 8.0, 700 mM NaCl, 15 mM imidazole) before elution with 300 mM imidazole. The purified protein samples were mixed with an equal volume of 2× SDS–PAGE loading buffer, boiled for 5 min at 100°C, and analyzed by electrophoresis on a 12% SDS–PAGE gel. Proteins were visualized using Coomassie Brilliant Blue staining.

Bacterial Treatment with Sodium Periodate

Sodium periodate treatment was performed as described previously, with slight modifications[33]. A 6 mL bacterial culture (OD600 = 0.6) was centrifuged at 2150 × *g* for 10 min, and the pellet was washed with 6 mL of TBS buffer. Cells were resuspended in 3 mL of TBS buffer and treated with 10 mM sodium

periodate (Sigma-Aldrich) for 1 h at 37°C. A 100 mM sodium periodate stock solution was prepared using Milli-Q water.

Fluorescence microscopy of GFP-tagged proteins

One milliliter of an overnight *H. pylori* culture with an OD600 of 0.8 was harvested by centrifugation at 6,000 × *g* for 5 min, washed once, and resuspended in fresh TBS buffer (50 mM Tris-HCl, pH 8.0, 10 mM $MgSO_4$, and 2 mM $CaCl_2$). One microgram of GFP-tagged protein was added to the cell suspension and incubated for 60 min at room temperature. After incubation, the cells were centrifuged at 6,000 × *g* for 5 min and washed twice with 1 mL of TBS. Finally, the pellet was resuspended in 20 µL of TBS, and 5 µL was fixed on a glass coverslip using paraformaldehyde (FUJIFILM Wako) prior to imaging. Imaging was performed using a confocal laser scanning microscope (LSM800, Carl Zeiss, Oberkochen, Germany). Images were processed using ZEN software (Carl Zeiss) and Adobe Photoshop (Adobe Systems, San Jose, CA, USA). Only linear adjustments of brightness were applied equally to all images.

Declarations

Competing interests

The all authors declare no competing interests.

Funding

This work was supported by the Astellas Foundation for Research on Metabolic Disorders (2023A3542), the Oita University President's Strategic Discretionary Funds, and the JSPS Bilateral Program (JPJSBP120257417) to H.M.; the joint research program of the Research Center for Global and Local Infectious Diseases, Oita University (2025A03) to K.K.; the Japan Agency for Medical Research and Development (AMED) [Research Program on Emerging and Reemerging Infectious Diseases (JP25fk0108732) to T.S.; Adopting Sustainable Partnerships for Innovative Research Ecosystem (ASPIRE; 23836904 to Y.Y. and H.M.); and Science and Technology Research Partnership for Sustainable Development (SATREPS; 21357105 to Y.Y.)].

Author Contribution

S.P.: Investigation, formal analysis, data curation, visualization, writing – original draft; T.M.: Methodology (phage and protein purification), supervision (protein and phage purification); R.I.-A.: Formal analysis (prophage genome sequencing and analysis); B.S.: Formal analysis (bacteriophage genome sequencing and analysis); S.O.: Investigation (electron microscopy sample preparation); M.K.: Investigation (electron microscopy), visualization; H.D.Q.D. and V.V.K.: Resources (provided *H. pylori* strains); T.O.: Resources (provided the parental *H. pylori* strain used as the phage host) and contributed to the interpretation of the data; T.S.: Investigation (electron microscopy), visualization, supervision (electron microscopy work);

Y.Y.: Resources (provided *H. pylori* strains, including prophage), supervision (sequencing work); K.K.: Conceptualization (initial proposal of the study), methodology (phage experimental strategy), technical guidance; H.M.: Conceptualization, supervision, formal analysis (with S.P.), data curation, writing – review, and editing. All authors have reviewed and approved the final manuscript.

Acknowledgement

We are grateful to Dr. Aa Haeruman Azam for valuable suggestions on phage replication kinetics experiments and to Mr. Jay Patel for insightful comments on phage genome assembly and subsequent analysis. We also thank all members of the Mimuro laboratory for their technical support.

Data Availability

All the data generated during this study are provided with this article.

The genome sequence of the bacteriophage generated in the current study has been deposited in the NCBI database under accession number PX985144.

References

1. Hooi, J. K. Global prevalence of Helicobacter pylori infection: systematic review and meta-analysis. *Gastroenterology* **153**, 420–429 (2017).
2. Sugano, K. *et al.* Kyoto global consensus report on Helicobacter pylori gastritis. *Gut* **64**, 1353–1367 (2015).
3. Malfertheiner, P. *et al.* Management of Helicobacter pylori infection—the Maastricht V/Florence consensus report. *Gut* **66**, 6–30 (2017).
4. Prashar, A., Capurro, M. I. & Jones, N. L. Under the radar: strategies used by Helicobacter pylori to evade host responses. *Annu. Rev. Physiol.* **84**, 485–506 (2022).
5. Tshibangu-Kabamba, E. & Yamaoka, Y. Helicobacter pylori infection and antibiotic resistance—from biology to clinical implications. *Nat. Rev. Gastroenterol. Hepatol.* **18**, 613–629 (2021).
6. Gandon, S. Why be temperate: lessons from bacteriophage λ. *Trends Microbiol.* **24**, 356–365 (2016).
7. Salmond, G. P. & Fineran, P. C. A century of the phage: past, present and future. *Nat. Rev. Microbiol.* **13**, 777–786 (2015).
8. Vale, F. F. *et al.* Genomic structure and insertion sites of Helicobacter pylori prophages from various geographical origins. *Sci. Rep.* **7**, 42471 (2017).
9. Ferreira, R. *et al.* Characterization and genomic analysis of a new phage infecting Helicobacter pylori. *Int. J. Mol. Sci.* **23**, 7885 (2022).

10. Uchiyama, J. *et al.* Characterization of Helicobacter pylori bacteriophage KHP30. *Appl. Environ. Microbiol.* **79**, 3176–3184 (2013).
11. Iwamoto, M. *et al.* Analysis of the life cycle of Helicobacter pylori bacteriophage KHP40 belonging to the genus Schmidvirus. *FEMS Microbiol. Lett.* **371**, 082 (2024).
12. Luo, C. H., Chiou, P. Y., Yang, C. Y. & Lin, N. T. Genome, integration, and transduction of a novel temperate phage of Helicobacter pylori. *J. Virol.* **86**, 8781–8792 (2012).
13. Phuc, B. H. *et al.* Helicobacter pylori type 4 secretion systems as gastroduodenal disease markers. *Sci. Rep.* **11**, 4584 (2021).
14. Arndt, D. *et al.* PHASTER: a better, faster version of the PHAST phage search tool. *Nucleic Acids Res.* **44**, 16–21 (2016).
15. Kamiya, R. *et al.* Acid-stable capsid structure of Helicobacter pylori bacteriophage KHP30 by single-particle cryoelectron microscopy. *Structure* **30**, 300–312.e3 (2022).
16. Bouras, G. *et al.* Pharokka: a fast scalable bacteriophage annotation tool. *Bioinformatics* **39**, btac776 (2023).
17. Moraru, C., Varsani, A. & Kropinski, A. M. VIRIDIC—A Novel Tool to Calculate the Intergenomic Similarities of Prokaryote-Infecting Viruses. *Viruses* **12**, 1268 (2020).
18. Gilchrist, C. L. M. & Chooi, Y.-H. clinker & clustermap.js: automatic generation of gene cluster comparison figures. *Bioinformatics* **37**, 2473–2475 (2021).
19. Nanda, A. M., Thormann, K. & Frunzke, J. Impact of spontaneous prophage induction on the fitness of bacterial populations and host-microbe interactions. *J. Bacteriol.* **197**, 410–419 (2015).
20. Ailloud, F., Estibariz, I. & Suerbaum, S. Evolved to vary: genome and epigenome variation in the human pathogen Helicobacter pylori. *FEMS Microbiol. Rev.* **45**, 042 (2021).
21. Oksanen, H. M., Poranen, M. M. & Bamford, D. H. Bacteriophages: Lipid-containing. in *Encyclopedia of Life Sciences* (Wiley, 2010). doi:10.1002/9780470015902.a0000779.pub2.
22. Laurinavičius, S., Bamford, D. H. & Somerharju, P. Transbilayer distribution of phospholipids in bacteriophage membranes. *Biochim. Biophys. Acta BBA-Biomembr.* **1768**, 2568–2577 (2007).
23. Dunstan, R. A. *et al.* Epitopes in the capsular polysaccharide and the porin OmpK36 receptors are required for bacteriophage infection of Klebsiella pneumoniae. *Cell Rep.* **42**, (2023).
24. Azam, A. H. *et al.* Selective bacteriophages reduce the emergence of resistant bacteria in bacteriophage-antibiotic combination therapy. *Microbiol. Spectr.* **12**, e00427-23 (2024).
25. Wick, R. R. *et al.* Trycycler: consensus long-read assemblies for bacterial genomes. *Genome Biol.* **22**, 266 (2021).
26. Wick, R. R. & Holt, K. E. Polypolish: Short-read polishing of long-read bacterial genome assemblies. *PLOS Comput. Biol.* **18**, e1009802 (2022).
27. McNair, K., Zhou, C., Dinsdale, E. A., Souza, B. & Edwards, R. A. PHANOTATE: a novel approach to gene identification in phage genomes. *Bioinformatics* **35**, 4537–4542 (2019).

28. Lowe, T. M. & Eddy, S. R. tRNAscan-SE: A Program for Improved Detection of Transfer RNA Genes in Genomic Sequence. *Nucleic Acids Res.* **25**, 955–964 (1997).
29. Steinegger, M. & Söding, J. MMseqs2 enables sensitive protein sequence searching for the analysis of massive data sets. *Nat. Biotechnol.* **35**, 1026–1028 (2017).
30. Terzian, P. *et al.* PHROG: families of prokaryotic virus proteins clustered using remote homology. *NAR Genomics Bioinforma.* **3**, lqab067 (2021).
31. Liu, B., Zheng, D., Zhou, S., Chen, L. & Yang, J. VFDB 2022: a general classification scheme for bacterial virulence factors. *Nucleic Acids Res.* **50**, D912–D917 (2022).
32. Alcock, B. P. *et al.* CARD 2023: expanded curation, support for machine learning, and resistome prediction at the Comprehensive Antibiotic Resistance Database. *Nucleic Acids Res.* **51**, D690–D699 (2023).
33. Serian, D. *et al.* Characterization of Temperate LPS-Binding Bordetella avium Phages That Lack Superinfection Immunity. *Microbiol. Spectr.* **11**, e03702-22 (2023).

Figures

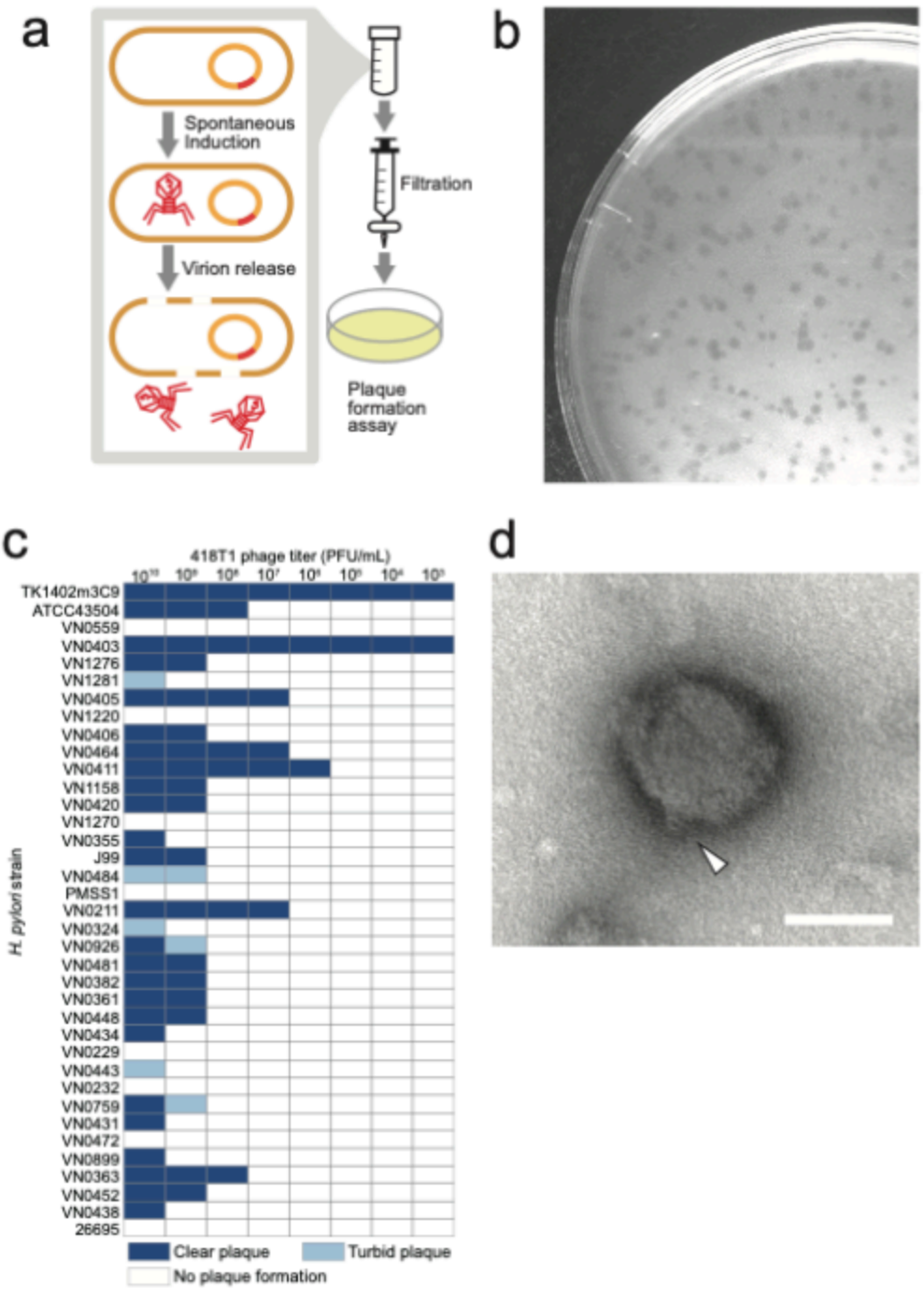


Figure 1

Isolation, host range, and morphological characterization of bacteriophage 418T1.

(a) Schematic diagram showing spontaneous prophage induction from the *H. pylori* VN0418 strain. **(b)** Host range determination of bacteriophage 418T1 against 38 *H. pylori* strains. Serial dilutions of phage lysate (10^{10} to 10^{3} PFU/mL) were spotted onto bacterial lawns. Blue indicates plaque formation (susceptible), white indicates no plaques (resistant), and light blue indicates turbid plaques. **(c)** Representative image showing clear plaques formed by bacteriophage 418T1 on *H. pylori*strain

TK1402m3C9. **(d)** Transmission electron micrograph of negatively stained 418T1 phage particles showing a spherical head with a short tail. White arrowhead indicates the short tail-like structure. Scale bar, 50 nm.

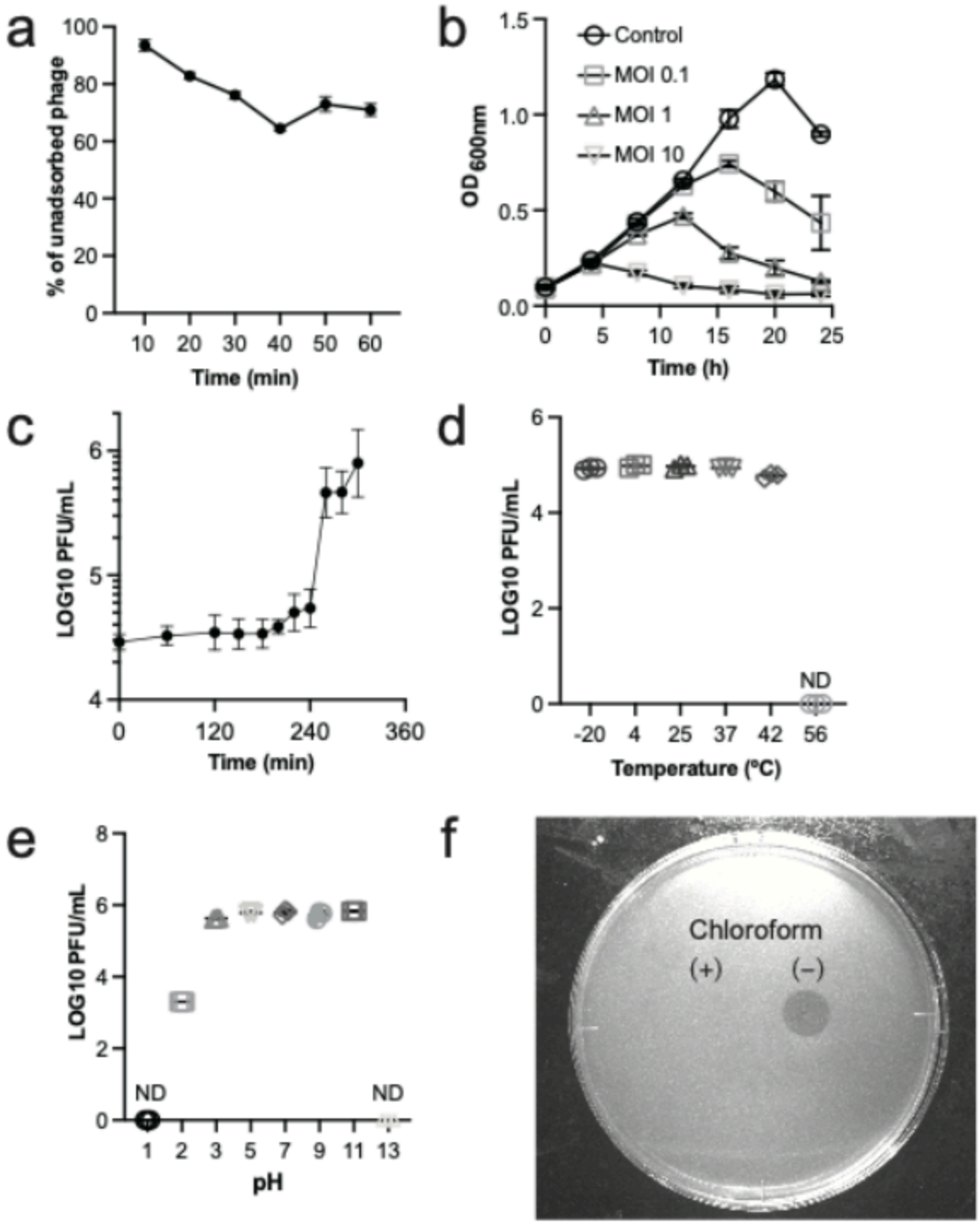


Figure 2

Infection and stability characteristics of bacteriophage 418T1.

(a) Adsorption kinetics of bacteriophage 418T1 on *H. pylori* strain TK1402m3C9. The percentage of unadsorbed phage particles remaining in the supernatant was measured at the indicated time points

following infection at an MOI of 0.001. A representative experiment from three independent experiments is shown. Data represent the mean ± SD, n = 3. **(b)** Lytic activity of bacteriophage 418T1 at different multiplicities of infection (MOI 0.1, 1, and 10). Bacterial growth was monitored by measuring OD600 over 24 h. Uninfected cultures served as controls. Data represent the mean ± SD, n = 3. **(c)** One-step growth curve of bacteriophage 418T1. Samples were collected at regular intervals for 300 min. The latent period was defined as the time prior to the sharp increase in phage titer. Data represent the mean ± SD, n = 3. **(d)** Thermal stability of bacteriophage 418T1 following incubation at −20°C, 4°C, 25°C, 37°C, 42°C, and 56°C for 60 min. Phage titers were determined by plaque assay. A representative experiment from three independent experiments is shown. Data represent the mean ± SD, n = 3. **(e)** pH stability of bacteriophage 418T1 following incubation at pH 1, 2, 3, 5, 7, 9, 11, and 13 for 60 min at room temperature. Phage titers were determined by plaque assay. A representative experiment from three independent experiments is shown. Data represent the mean ± SD, n = 3. **(f)** Chloroform sensitivity of bacteriophage 418T1. Ten µL of 10^8 PFU phage suspension was spotted onto bacterial lawns after chloroform treatment (left) or without treatment (right).

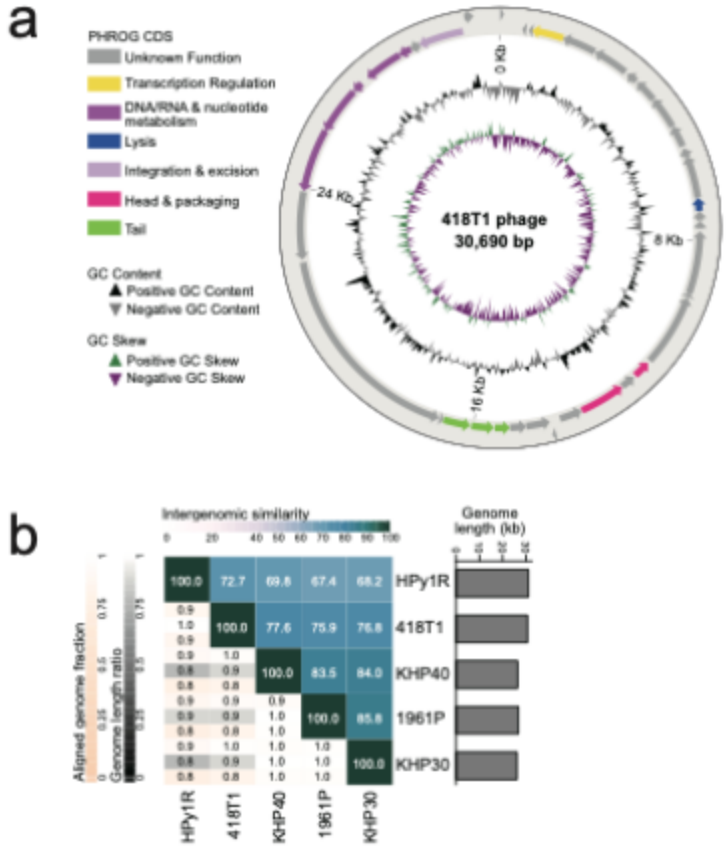


Figure 3

Genomic organization and comparative analysis of bacteriophage 418T1.

(a) Genome map of bacteriophage 418T1 (30,690 bp). Arrows represent predicted open reading frames (ORFs), colored by functional categories. The outer track indicates genome coordinates, and the inner track shows GC content. **(b)** Intergenomic similarity matrix comparing 418T1 with related *H. pylori*

bacteriophages (KHP30, KHP40, 1961P, and HPy1R), calculated using the VIRIDIC tool. Values represent percent nucleotide similarity.

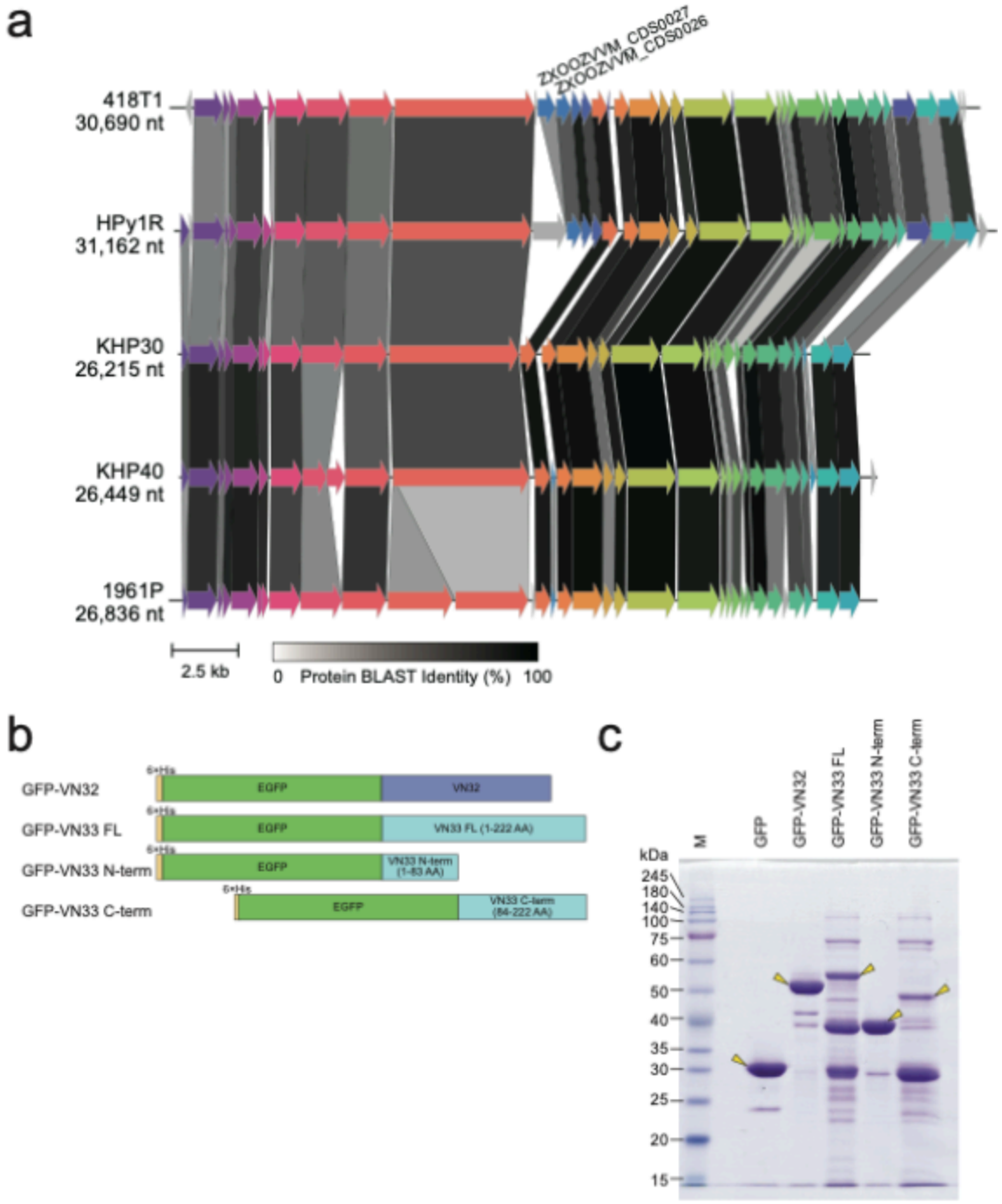


Figure 4

Tail fiber protein expression.

(a) Comparative genome alignment of bacteriophage 418T1 with related *H. pylori* phages generated using the clinker. Homologous regions are connected by shaded areas, with shading intensity representing protein BLAST identity (%). Predicted ORFs are shown as arrows. Tail fiber protein genes (ZXOOZVVM_CDS0026 and ZXOOZVVM_CDS0027) are highlighted. **(b)**Schematic representation of

recombinant tail fiber protein constructs used in this study. Full-length VN32 (184 amino acids) and VN33 (222 amino acids) were expressed with N-terminal His-GFP tags. Two truncated variants of VN33 were generated: the N-terminal domain (amino acids 1–83) and the C-terminal domain (amino acids 84–222), each fused to an N-terminal GFP tag. **(c)** SDS-PAGE analysis of purified recombinant proteins. M, molecular weight markers (kDa); GFP-VN32 (49.4 kDa); GFP-VN33 FL (53.6 kDa); GFP-VN33 N-term (37.7 kDa); GFP-VN33 C-term (44.7 kDa). The bands corresponding to the expected molecular weight of each recombinant protein in each lane are indicated by yellow arrowheads. The original uncropped gel image is shown in Supplementary Figure 1.

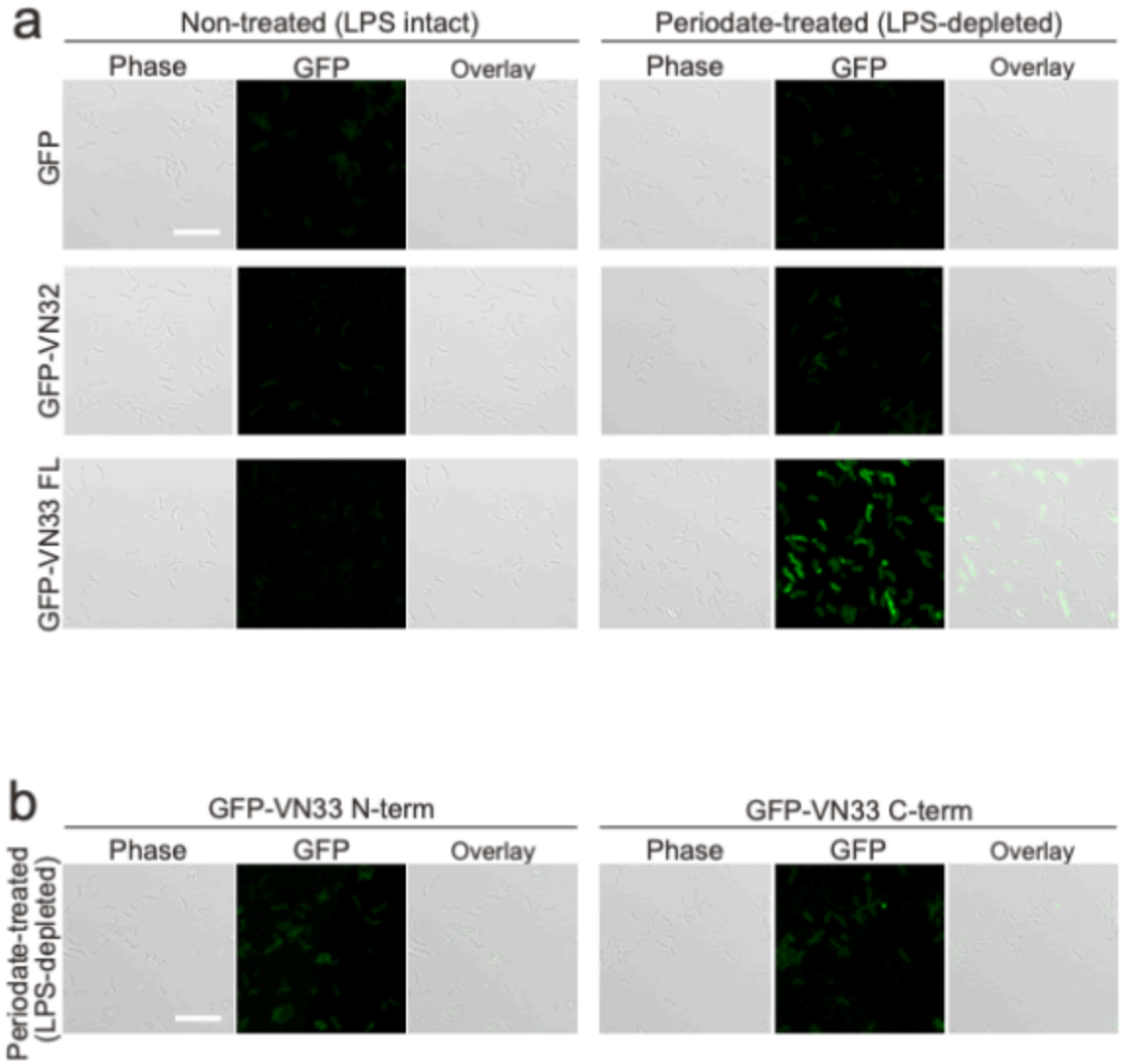


Figure 5

Binding of GFP-fused tail fiber protein to *H. pylori* is dependent on LPS.

(a) Representative confocal fluorescence microscopy images showing binding of GFP, GFP-VN32, and GFP-VN33 FL (Full length) to *H. pylori*under non-treated (LPS intact) and periodate-treated (LPS-depleted) conditions. GFP (green), phase-contrast images, and merged overlays are shown. **(b)** Binding of N-terminal (GFP-VN33 N-term) and C-terminal (GFP-VN33 C-term) fragments of VN33 fused to GFP

(GFP-VN33 N-term and GFP-VN33 C-term, respectively) to LPS-depleted *H. pylori* following periodate treatment. Scale bars, 10 μm.

Supplementary Files

This is a list of supplementary files associated with this preprint. Click to download.

- Supplementarydata260303CLEAN.docx